RSC Advances

PAPER

View Article Online
View Journal | View Issue

Cite this: *RSC Adv.*, 2014, **4**, 43890

Efficient oral insulin delivery by dendronized chitosan: *in vitro* and *in vivo* studies

Piyasi Mukhopadhyay,[a] Kishor Sarkar,[a] Sourav Bhattacharya,[b] Roshnara Mishra[b] and P. P. Kundu*[a]

Received 23rd July 2014
Accepted 29th August 2014

DOI: 10.1039/c4ra07511k

www.rsc.org/advances

The development of efficient and bio-safe polymeric carriers for oral insulin delivery is a major thrust in biomedical research. In this paper, dendronized chitosan (DCTS) is prepared using a Michael-type addition reaction by grafting polyamidoamine (PAMAM) onto chitosan to improve its water solubility, pH sensitivity, and insulin encapsulation efficiency for enhanced bioavailability of the oral insulin. The self-assembled dendronized chitosan nanoparticles are prepared using a mild coacervation method, in which almost sub-spherically shaped nanoparticles of 85–150 nm size are produced, with an insulin encapsulation of approx. 95%. *In vitro* release study confirms a pH-sensitive and self-sustained release of insulin, where the oral administration of these nanoparticles exhibits a pronounced hypoglycemic effect in diabetic mice, producing a relative bioavailability of ~9.19%. As no systemic toxicity is observed with its peroral delivery, these DCTS nanoparticles can effectively serve as a promising device in the efficient administration of oral insulin.

1. Introduction

Oral insulin delivery remains a great challenge in the biomedical field due to several problems, such as the harsh acidic environment in the stomach, extensive enzymatic degradation by different proteolytic enzymes of the GI tract, and barriers presented by the mucosal surface and the tight junction in between the intestinal epithelial cells.[1] Despite remarkable advancements in oral insulin delivery for combating diabetes mellitus,[2] an efficient and satisfactory oral insulin delivery vehicle remains unavailable. Recently, biodegradable polymers such as protein- and polysaccharide-based nanoparticles have gained tremendous attention in pharmaceutical research as efficient drug delivery vehicles for controlled and targeted drug release, which aim to improve the therapeutic effects and also reduce the side effects of the formulated drugs.[3] Over the past few decades, chitosan has received appreciable interest among other polysaccharides for drug delivery due to its biodegradable, biocompatible, non-toxic and non-immunogenic properties.[1] Chitosan, isolated from chitin by alkaline hydrolysis, is a cationic, linear and partly acetylated (1 → 4)-2-amino-2-deoxy-β-D-glucan. Chitosan has a pK_a value of 6.5, and therefore, it is only soluble in acidic aqueous solutions such as formic, acetic, pyruvic, 10% citric and lactic acids and becomes cationic due to the protonation of its primary amine groups at pH < 6.5.[4] Therefore, positively charged chitosan can easily encapsulate negatively charged bio-macromolecules such as DNA or insulin *via* electrostatic interaction.[5,6] However, acidic solutions of chitosan may not be desirable in many applications, such as cosmetics, food and biomedicine.[4] Hence, successive modifications have been implemented to improve its water solubility, physicochemical and biochemical properties.[7–9]

On the other hand, a new class of synthetic polymers, the polyamidoamine (PAMAM) dendrimer, has gained considerable attention in biomedical research due to its water solubility, size uniformity, and highly branched nano-spherical architecture with precise molecular weight.[10,11] Moreover, full-generation cationic PAMAM dendrimers (amine terminated) can also form complexes with negatively charged biomolecules such as protein, DNA, RNA *etc.* by electrostatic interaction.[12] However, the severe toxicity of high-generation PAMAM dendrimers (with a high density of primary amine groups) limits its widespread application in the biomedical field.[13] Therefore, a chemical combination of chitosan with PAMAM may provide a novel biomaterial with improved water solubility, higher charge density and lower toxicity for efficient oral insulin delivery.

In our previous studies, we prepared *N*-maleated, chitosan-*graft*-PAMAM copolymer and PAMAM–chitosan conjugated through the naphthalimide moiety for efficient gene delivery with improved water solubility and minimal toxicity.[5,14] However, it was observed during the preparation of *N*-(4-bromonaphthalimide)-chitosan that a higher molar ratio of naphthalimide to chitosan produced a water-insoluble product that was not soluble even after grafting of PAMAM; the water-insoluble product is not suitable for oral insulin delivery and

[a]*Department of Polymer Science and Technology, University of Calcutta, 92, A.P.C. Road, Kolkata-700009, India. E-mail: ppk923@yahoo.com; Fax: +91-2352-5106; Tel: +91-2352-5106*

[b]*Department of Physiology, University of Calcutta, 92, A.P.C. Road, Kolkata-700009, India*

may also cause systemic toxicity within the animal body. Therefore, in this work, we prepared a low-generation, conjugated chitosan through the *N*-carboxyethyl chitosan methyl ester intermediate for oral insulin delivery. In comparison to previously reported materials,[15,16] the graft copolymer in this article is unique with respect to its mode of preparation and properties. Furthermore, the preparation of PAMAM (G 2.0)-conjugated chitosan through the *N*-carboxyethyl chitosan methyl ester intermediate is advantageous, because it allows the conjugation of high-generation dendrimer on chitosan, thereby improving its water solubility. Finally, self-assembled nanoparticles were prepared with insulin, and physical characterization of the nanoparticles, together with their insulin loading capacity, insulin encapsulation efficiency, *in vitro* insulin release, *in vivo* pharmacological responses, insulin bioavailability and also their toxicity were investigated in detail in this article.

2. Materials and methods

2.1. Materials

Chitosan (molecular weight, 222 kDa and degree of deacetylation, DDA 82%) was obtained from Himedia, India. Low-molecular weight chitosan (25 kDa, DDA 82%) was prepared by oxidative degradation using sodium nitrite (Merck, India) at room temperature according to our previous method.[6] Ethylenediamine (EDA), methyl acrylate (MA), creatinine Merckotest kit and methanol were purchased from Merck, India. PAMAM dendrimer (G 2.0) was synthesized according to previous reports.[5,17] Insulin (bovine insulin, 27 USP units per mg) and alloxan monohydrate were purchased from Sigma-Aldrich. Bovine insulin ELISA kit, lactate dehydrogenase LDH (P-L) kit and micro-protein kit were purchased from LILAC Medicare Pvt. Ltd. and Crest Biosystems, India, respectively. Serum glutamate pyruvate transaminase (SGPT) ALAT (GPT)-LS kit and serum glutamate oxaloacetate transaminase (SGOT) AST (GOT)-LS kit were obtained from Piramal Health Care Limited, India. Multistix reagent strips were purchased from Siemens, India. All other chemicals were used as received.

Animals: Male Swiss albino mice (26 ± 2 g) (M s^{-1} Chakraborty Enterprise, Calcutta, India) were housed under a controlled environment (room temperature: 23 ± 2 °C, relative humidity: 60 ± 5%, 12 h day/night cycle) with a balanced diet and water *ad libitum*. All the animal experiments were approved by the animal ethical committee, Department of Physiology, University of Calcutta, in accordance with the guideline of the committee for the purpose of control and supervision of experiments on animals (CPCSEA Ref no.: 820/04/ac/CPCSEA dated 06.08.2004), Government of India.

2.2. Synthesis of dendronized chitosan

Dendronized chitosan was prepared by two consecutive steps; the preparation of *N*-carboxyethyl chitosan methyl ester (NCME) followed by conjugation of PAMAM dendrimer (G 2.0) with the NCME. *N*-carboxyethyl chitosan methyl ester was prepared according to the previous report with slight modification.[18] At first, chitosan was purified by re-precipitation method prior to the reaction.[6] Then, 1.0 g of purified chitosan was dissolved in 50 mL of 1% acetic acid solution under constant stirring for 30 min and diluted with 200 mL of ethyl alcohol. To this solution, methyl acrylate (10 equiv./NH_2 of chitosan) was added slowly, and the reaction was further continued for 48 h at 25 °C. After that, the reaction mixture was concentrated to approx. 100 mL under reduced pressure to remove the excess methyl acrylate and solvent. The remaining mixture was dialyzed for 3 days against deionised water and lyophilized for another 3 days to obtain *N*-carboxyethylchitosan methyl ester.

To conjugate PAMAM dendrimer with NCME, *N*-carboxyethylchitosan methyl ester (100 mg) was dispersed in methyl alcohol (50 mL), and then, PAMAM (0.54 mmol: 1.0 equiv./CO_2Me) in MeOH (50 mL) was added to this suspension. The reaction mixture was allowed to stir at room temperature. After 3 days, the mixture was evaporated to dryness and dispersed in 0.2 M NaOH solution at room temperature for 2 h, dialyzed and finally lyophilized to get the final product, dendronized chitosan (DCTS), as presented in Fig. 1.

2.3. Characterization of polymer

Fourier transform infrared (FT-IR) analysis was carried out with ATR-FTIR (model-Alpha, Bruker, Germany) spectrometer, scanning from 4000 to 500 cm^{-1} for 42 consecutive scans at room temperature. Samples were mixed separately with KBr and pressed into pellets for measurements.

The ^1H nuclear magnetic resonance (^1H NMR) spectra were measured on a Bruker AV 3000 Supercon NMR system (Germany) at 500 MHz using D_2O/DCl and D_2O as solvent. Chemical shifts (δ) were reported in ppm using tetramethylsilane (TMS) as an internal reference.

The molecular weight of chitosan and its derivatives were measured by gel permeation chromatography (GPC). The GPC equipment consisted of ultrahydrogel 1000 (7.8 × 300 mm) column, 515 HPLC pump and 2414 RI detector (Waters, USA). The mobile phase was 0.1 M acetic acid/0.1 M sodium acetate buffer. Mobile phase and chitosan solution were filtered through a 0.45 μm filter (Millipore). The flow rate was maintained at 0.3 mL min^{-1}. The sample concentration was 0.3 mg mL^{-1}. Polyethylene glycol (Sigma-Aldrich) standards were used to calibrate the column. All data provided by the GPC system were analyzed using the Empower 2 software package.

2.4. Preparation of polymer/insulin self-assembled nanoparticles

Self-assembled nanoparticles were prepared by complex coacervation method according to our previous report.[6] Chitosan and dendronized chitosan were dissolved in 5 mM sodium acetate–acetic acid buffer solution at a pH of 5.5. Insulin was dissolved in 0.1 M HCl solution, and the pH of the solution was adjusted to 8.4 by 0.1 N Tris (hydroxymethyl) aminomethane solution. Then, equal volumes of polymer and insulin solution (1 mg mL^{-1}) were mixed at different weight ratios (0.5 : 1, 1 : 1 and 2 : 1), immediately vortexed for 15–30 seconds and allowed

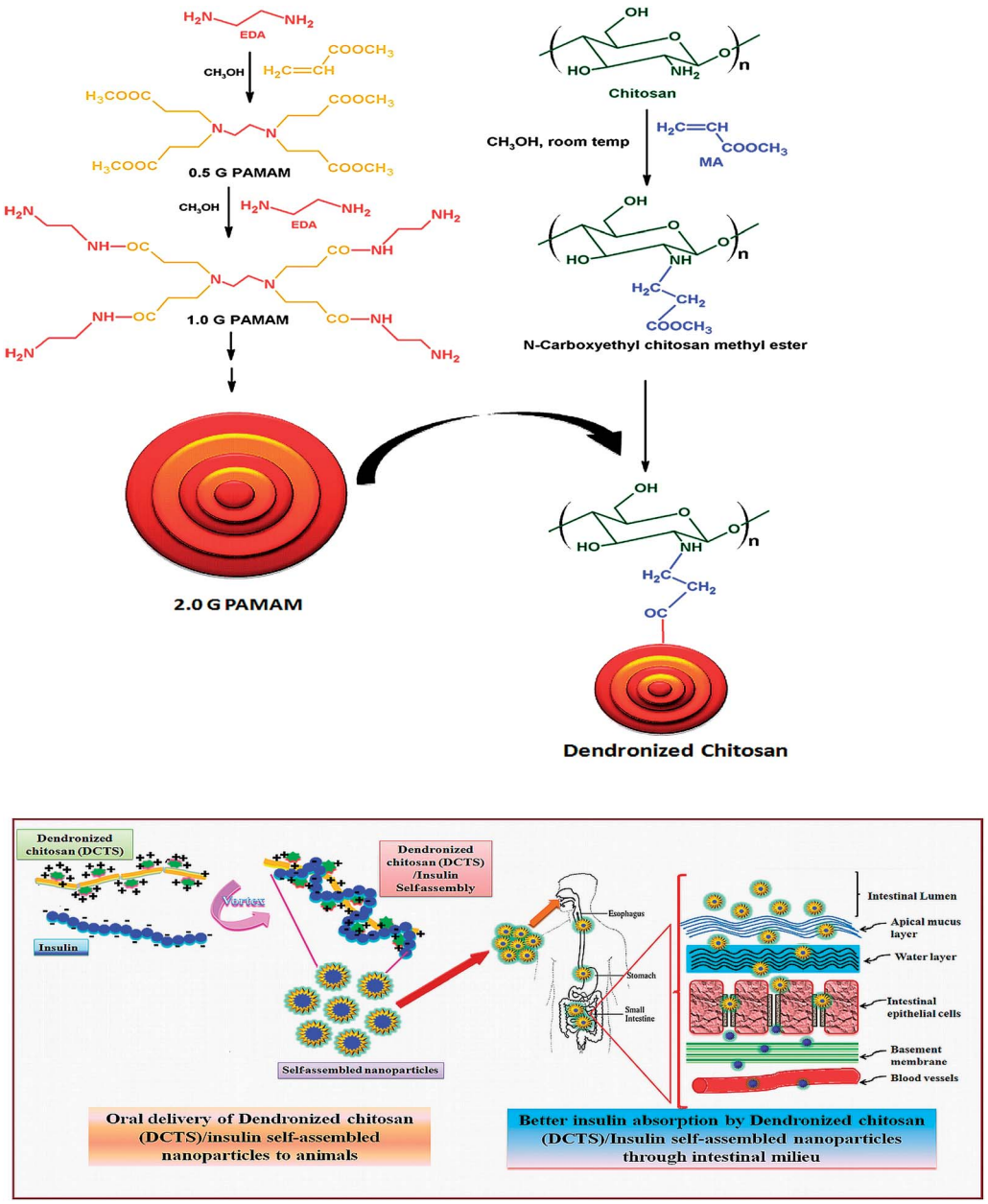

Fig. 1 Synthesis of dendronized chitosan, preparation of dendronized chitosan and insulin self-assembled nanoparticles and their application in *in vivo* models.

to incubate at room temperature for another 20–30 min to form the self-assembled nanocomplexes.

2.5. Determination of particle size and zeta potential and morphological analysis of polymer/insulin self-assembled nanoparticles

Particle size and zeta potential of polymer/insulin complexes at different weight ratios were measured in DLS equipped with Zetasizer. The solutions were filtered through a 0.45 μm filter (Millipore) prior to the experiment to avoid the influence of dust on the reliability of results. The intensity of autocorrelation was measured at a scattering angle (θ) of 173° with Zetasizer Nano ZS (Malvern Instrument, UK) digital autocorrelator at 37 °C. The mean diameter was obtained by the Stokes–Einstein relationship.

The size and morphology of the nanocomplexes were also characterized by AFM (Nanoscope IV Bioscopet, Digital Instruments, Veeco) and SEM (Carl Zeiss EVO 18, Germany). 1–2 μL of samples containing complexes in acetate buffer was deposited onto the centre of a freshly split, untreated mica disk and glass slide for AFM and SEM, respectively. AFM imaging was conducted with silicon nitride tip in tapping mode and at a scan speed of 1 Hz at ambient condition. Before SEM observation, the samples were fixed on an aluminium stub and coated with gold by an ion sputter coater (Hitachi, Japan, Model-E1010) for

6 min. An acceleration voltage of 20 kV was used during the scanning.

2.6. Insulin loading capacity and insulin encapsulation efficiency of self-assembled nanoparticles

After polymer/insulin complex formation at different weight ratios, the solution mixture was centrifuged at 14 000 rpm min^{-1} for 30 min at 4 °C. The clear supernatant was analyzed for insulin content using UV-vis spectrophotometer (OPTIGEN POP BIO, Mecasys Co. Ltd., Korea) at 280 nm. All experiments were done in triplicate to calculate insulin loading capacity (LC) and encapsulation efficiency (EE) by the following formula:[4,6]

$$\text{LC}\ (\%) = \frac{\text{total amount of insulin} - \text{free insulin in the supernatant}}{\text{weight of the nanoparticles}} \times 100 \quad (1)$$

$$\text{EE}\ (\%) = \frac{\text{total amount of insulin} - \text{free insulin in the supernatant}}{\text{total amount of insulin}} \times 100 \quad (2)$$

2.7. *In vitro* insulin release profile from the self-assembled nanoparticles

To determine the insulin release profile and pattern, the polymer/insulin complexes were immersed in simulated gastric fluid (SGF), pH 1.2, and simulated intestinal fluid (SIF), pH 7.4, with mild agitation. At specific time intervals, the samples were centrifuged, and an aliquot from each sample was taken out. The concentration of the released insulin was determined using a UV-vis spectrophotometer at 280 nm. To determine the insulin release mechanism, the *in vitro* insulin release data were fitted to standard zero-order, first-order, Higuchi and Korsmeyer–Peppas models,[19–21]

$$\frac{M_t}{M_\infty} = Kt^n \quad (3)$$

where M_t and M_∞ are the absolute amounts of insulin released at time (t); K is a constant showing the structural and geometric characteristics of the device; n is the release exponent reflecting the diffusion mechanism. Values of the release exponent (n) = 0.45, $0.45 < n < 0.89$ and 0.89 indicate Fickian (Case I) diffusion, non-Fickian (anomalous) transport, and diffusion and zero-order (Case II) transport, respectively.

2.8. Mucoadhesion studies of self-assembled nanoparticles in animal model

Mucoadhesion studies were carried out on small intestine tissue freshly excised from mice according to our previously described method.[21] Saline was flushed through freshly excised intestinal tissue to remove luminal contents, and the sample was placed in a glass support with the help of adhesive. The polymer/insulin self-assembled nanoparticles (freeze dried) were uniformly spread and allowed to interact with the intestinal mucosal lining for 10–15 min and then were mounted at an angle of 45° on a platform under a constant flow rate (10 mL min^{-1}) of phosphate buffer (pH 7.4). The percentage of nanoparticle adherence was calculated by comparing the weight of adhered nanoparticles to the initial weight of nanoparticles taken for the experiment.

2.9. *In vivo* pharmacological response of polymer/insulin self-assembled nanoparticles

Diabetes was induced in mice (26 ± 2 g) according to our previous reports.[6,21] To assess the *in vivo* pharmacological response, the following formulations were orally administered to diabetic mice ($n = 6$ in each group): group I: oral insulin solution (50 IU kg^{-1} b.w.), group II: oral chitosan/insulin nanoparticles (50 IU kg^{-1} b.w.), group III: oral DCTS/insulin self-assembled nanoparticles (50 IU kg^{-1} b.w.) and group IV (control): subcutaneous injection of insulin solution (5 IU kg^{-1} b.w.). The blood glucose level was checked at regular intervals (1 h) using a Bayer glucose meter.

2.10. Measurement of serum insulin and relative bioavailability

Again, the concentration of serum insulin was measured following peroral treatment of insulin-loaded nanoparticles. The following formulations were administered to diabetic mice ($n = 6$, each group): group I, oral insulin solution (50 IU kg^{-1} b.w.); group II, oral chitosan/insulin nanoparticles (50 IU kg^{-1} b.w.); group III, oral DCTS/insulin self-assembled nanoparticles (50 IU kg^{-1} b.w.); and group IV (control), SC injection of insulin solution (5 IU kg^{-1} b.w.). The blood serum was separated by centrifugation for 10 min at 5000 rpm and at 4 °C, and insulin concentrations were quantified using enzyme-linked immunosorbent assay (ELISA). The relative bioavailability (RA) of insulin was calculated using the following formula:[21,22]

$$\text{Relative bioavailability (RA)} = \frac{\text{AUC}_{(\text{Oral})} \times \text{DOSE}_{(\text{Sc})}}{\text{AUC}_{(\text{Sc})} \times \text{DOSE}_{(\text{Oral})}} \times 100\% \quad (4)$$

where AUC is the total area under the curve of plasma insulin concentration *versus* time.

2.11. *In vivo* toxicity assay of the polymers

Acute toxicity studies were conducted with peroral treatment of chitosan and dendronized chitosan (DCTS) nanoparticles at a dose of 300 mg kg^{-1} b.w. per day in mice. Experimental animals were divided into the following three groups ($n = 6$): Group I (control), only 0.5 mL 0.9% saline perorally; group II, chitosan nanoparticles (300 mg kg^{-1} b.w. per day) orally; group III, DCTS nanoparticles (300 mg kg^{-1} b.w. per day) orally.

On the next day, urine was collected, and the animals were anesthetized to collect blood from the retro-orbital vein. Serum was separated and stored at −20 °C for assessment of different biochemical parameters.

2.11.1. Liver function test. The serum glutamate pyruvate transaminase (SGPT), serum glutamate oxaloacetate

transaminase (SGOT) and lactate dehydrogenase activity (LDH) were estimated to analyse hepato-toxicity in the treated mice.

2.11.2. Nephro-toxicity test. Urine samples were analyzed for quantitative measurement of creatinine (serum and urine), micro-protein and urea to evaluate the nephro-toxicity in the treated animals. Again, urine samples were qualitatively analyzed using multistix reagent strips.

2.11.3. Pathohistological diagnosis. For pathohistological diagnosis, liver and kidney were fixed in 10% phosphate buffered formalin, and tissue sections were stained with haematoxylin and eosin (H&E) and observed under microscope.

2.12. Statistical analysis

The acute toxicity results are expressed as mean ± SE, $n = 6$. The significance level was determined by one-way ANOVA following Tukey's post hoc test. $p < 0.05$ was considered as significant.

3. Results and discussion

3.1. Characterization of polymers

FTIR spectra of the polymers are shown in Fig. 2. The FTIR spectrum of chitosan (Fig. 2a) shows the basic characteristic peaks at 3427 cm^{-1} (O–H stretch and N–H stretch overlap), 2922 cm^{-1} and 2859 cm^{-1} (asymmetric and symmetric stretching of C–H, respectively), 1652 cm^{-1} (NH–CO(I) stretch), 1597 cm^{-1}(N–H bend), 1154 cm^{-1}(bridge –O stretch), and 1092 cm^{-1} (C–O stretch).[4] Fig. 2b shows the FTIR spectrum of *N*-carboxyethylchitosan methyl ester. A new strong absorption peak at 1728 cm^{-1} appears due to the stretching vibration of the carbonyl bond (C=O) of the ester group. The FTIR spectrum of PAMAM dendrimer (G 2.0, Fig. 2c) shows the strong absorption peaks at 3281 cm^{-1} and 1545 cm^{-1} corresponding to the N–H bond of primary amine (–NH_2) groups. The strong absorption peak at 1636 cm^{-1} is associated with the amide N–H bond in the –CONH group. From Fig. 2d, it is found that the intensity of absorption peaks at 1651 cm^{-1} (NH CO(I) stretch), 3282 cm^{-1}, and 1557 cm^{-1} (N–H stretching and bending, respectively) increased after reaction of the PAMAM dendrimer (G 2.0) with the *N*-carboxyethylchitosan methyl ester, and the peak for ester group at 1728 cm^{-1} disappeared, indicating the formation of dendronized chitosan.

The ^{1}H NMR spectra of chitosan, *N*-carboxyethylchitosan methyl ester and DCTS are shown in Fig. 3. In Fig. 3a, typical peaks at 3.4–4.0 ppm are assigned to the glucosamine unit (H3, H4, H5, H6) of chitosan; the peak at 3.1 ppm is responsible for H2; the peak at 2.1 ppm is assigned to the methyl protons of the *N*-acetyl group. After the reaction between chitosan and methyl acrylate, a new triplet peak appeared at 2.2–2.7 ppm in the NMR spectrum of *N*-carboxyethylchitosan methyl ester (Fig. 3b); this peak is attributed to the methylene protons of methyl ester. After further reaction of PAMAM dendrimer (G 2.0) with *N*-carboxyethyl chitosan methyl ester, the peak for the methylene proton of the methyl ester disappeared, and another new broad

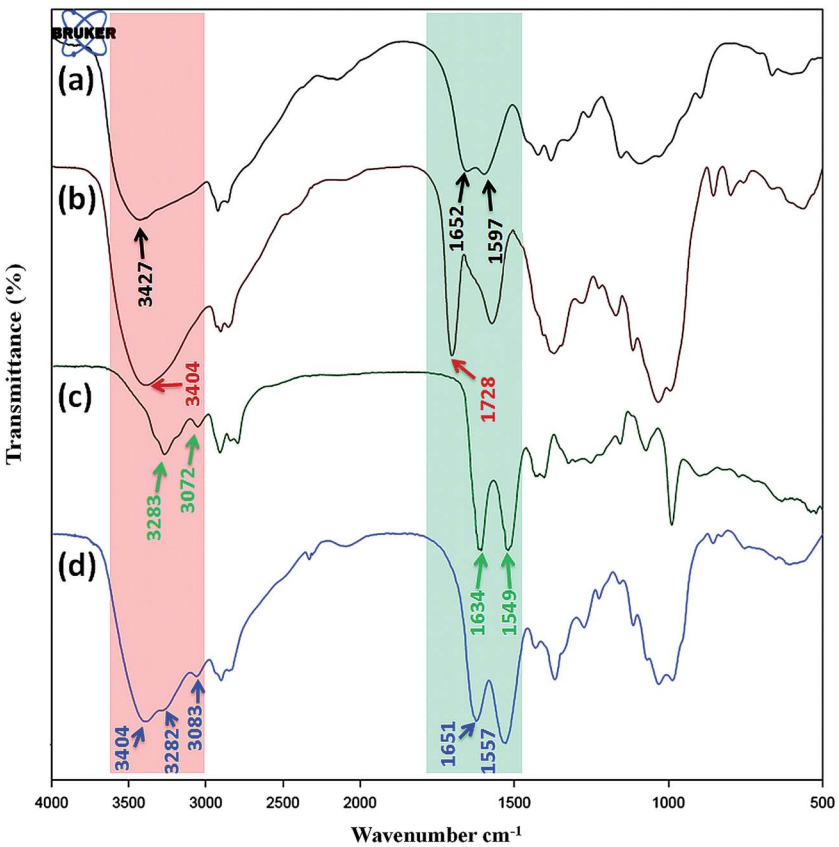

Fig. 2 The FT-IR spectra of (a) chitosan, (b) *N*-carboxyethylchitosan methyl ester, (c) PAMAM (G 2.0) and (d) DCTS.

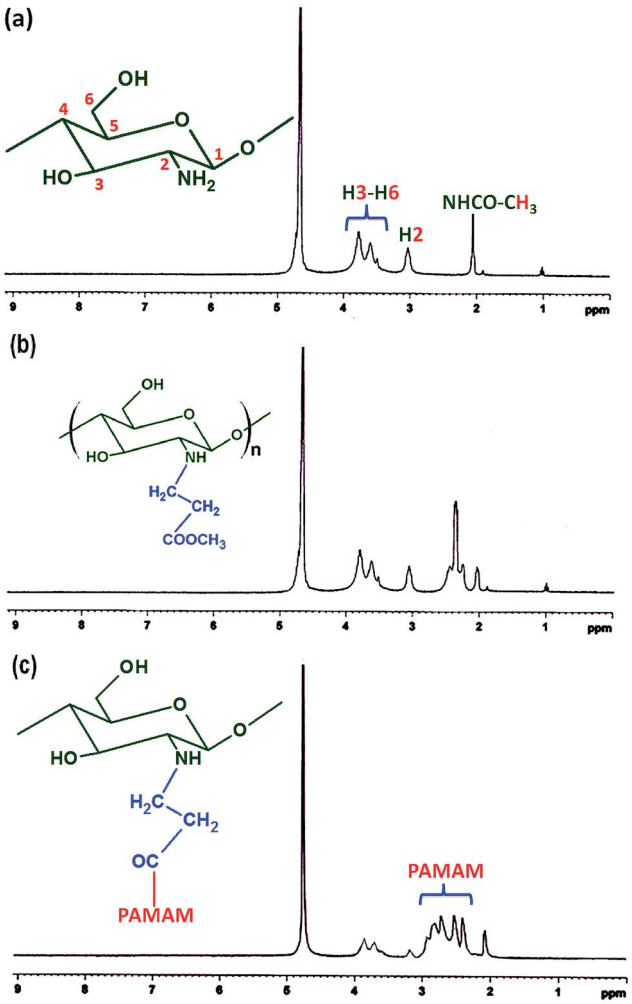

Fig. 3 The ^{1}H NMR spectra of (a) chitosan, (b) *N*-carboxyethylchitosan methyl ester, and (c) DCTS.

peak with multiplicity appeared at 2.2–3.0 ppm, indicating the formation of dendronized chitosan (Fig. 3c).

3.2. Molecular weight and solubility

The molecular weight and solubility of chitosan and its derivatives are shown in Table 1. To improve the water solubility of chitosan, CTS was depolymerised by oxidation using nitrous acid, and the molecular weight of native chitosan was decreased from 222 kDa to 25 kDa. However, its molecular weight was slightly increased from 25 kDa to 37.4 kDa and 41.86 kDa due to the incorporation of methyl acrylate and PAMAM dendrimer (G 2.0), respectively, on the chitosan backbone. On one hand, the water solubility of chitosan was increased after conjugation of PAMAM dendrimer with chitosan because of the augmentation of primary amine groups of dendronized chitosan. On the other hand, we got insoluble products (data not shown) when we used an equivalent or lower amount of PAMAM dendrimer during the conjugation of *N*-carboxyethyl chitosan methyl ester (NCME) and PAMAM dendrimer. This is possible due to intermolecular crosslinking. To avoid this, we used an excess amount of PAMAM dendrimer compared to the methyl ester of chitosan. When the lower or equivalent amount of PAMAM was used, the free primary amine groups of the chitosan methyl ester might have reacted with other chitosan methyl esters and resulted in an insoluble crosslinked product. However, when the PAMAM dendrimer is in excess, its reaction with the chitosan methyl ester is preferred due to the smaller size of PAMAM dendrimer in comparison to the size of the chitosan methyl ester, and this reaction results in water-soluble dendronized chitosan. Similar results have been observed in earlier reports.[5]

3.3. Particle size, zeta potential and morphology of polymer/insulin self-assembled nanoparticles

An appropriate particle size of polycation/insulin nanocomplexes is a very important parameter for oral insulin delivery, as particles below 1000 nm in diameter are reported to be more desirable for better absorption through the intestinal tract.[23] The diameters of the self-assembled nanoparticles at various polycation/insulin ratios were measured by dynamic light scattering (DLS), and the average particle size is shown in Fig. 4a. It is observed that the average particle size of DCTS/insulin nanocomplexes at different weight ratios is 80–175 nm, whereas the average particle size of unmodified chitosan/insulin nanoparticles at similar weight ratios are comparatively larger and in the range of 150–475 nm.[6] This may be attributed to the availability of more positive charges on the surface of DCTS (due to grafting of PAMAM) compared to the native chitosan, thereby tightly entrapping the excess amount of insulin (negatively charged) to form smaller nanoparticles. Again, a slight increase in particle size is documented with further augmentation in

Table 1 Molecular weight and solubility of chitosan and modified chitosan[a]

Polymeric compound	Average molecular weight (M_w) (kDa)	Solubility		
		H_2O	0.1 M HCl	0.1 M NaOH
Chitosan	222	I	S	I
Depolymerized chitosan	25	I	S	I
N-Carboxyethylchitosan methyl ester	37.4	P	I	P
PAMAM (G 2.0)	1.321	S	S	I
N-Carboxyethylchitosan methyl ester grafted PAMAM (G 2.0) or dendronized chitosan	41.86	S	S	I

[a] I = insoluble, P = partly soluble, S = soluble.

polymer concentration; this may be attributed to the strong repulsion between excess positive charges available on the surface of polymeric molecules after complete electrostatic interaction with the negatively charged insulin. Similar results are also found in our previous study.[6] In previous studies, chitosan nanoparticles (265–387 nm) were used for oral insulin delivery,[24] and other polymeric systems with a particle size of 200 nm have also been reported for insulin delivery.[22] In the present article, the particle size is comparable to earlier reports.

The zeta potential values of the self-assembled nanoparticles are shown in Fig. 4b. The zeta value of insulin is found to be −10.06 mV, whereas a sharp increase in zeta potential of the chitosan/insulin and DCTS/insulin nanoparticles at 0.5 : 1 weight ratio is observed, at +2.83 mV and +6.82 mV, respectively. Again, with an increase in weight ratio to 1 : 1 and 2 : 1, the zeta value is found to further increase to +8.9 mV and +18.44 mV for chitosan/insulin and +16.46 mV and +25.71 mV for DCTS/insulin nanoparticles, respectively (Fig. 4b). The zeta potential of the nanoparticles is positive, although insulin is negatively

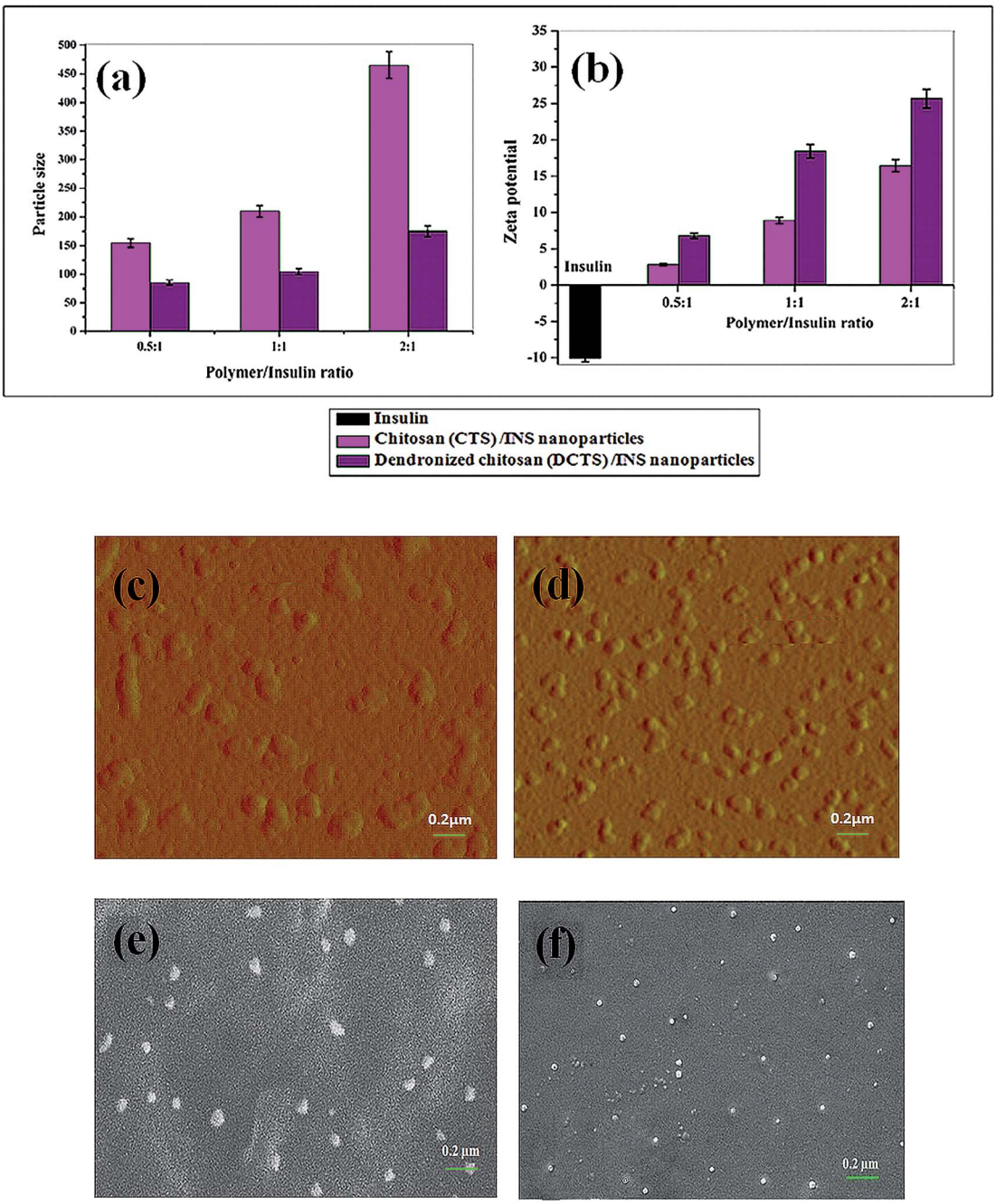

Fig. 4 (a) Particle size, (b) zeta potential, (c) AFM images of chitosan/insulin and (d) AFM images of DCTS/insulin nanoparticles, (e) SEM images of chitosan/insulin and (f) SEM images of DCTS/insulin nanoparticles.

charged; this has happened due to the neutralization of all the negative charges on the insulin molecules by the cationic charges on polymers (chitosan and DCTS) *via* electrostatic interaction (Fig. 4b). As DCTS carries comparatively more surface cationic charges than native chitosan, the zeta potential of DCTS/insulin nanoparticles is found to be more positive as compared to native chitosan/insulin nanocomplexes. Therefore, the positive zeta potential value of nanoparticles can provide prolonged attachment with the negatively charged intestinal mucus layer, facilitating sustained release of encapsulated insulin by increasing their stability with effective protection against self-aggregation.

Both atomic force microscopy and scanning electron microscopy were utilized to observe the morphology and size of the prepared nanocomplexes. Fig. 4c and d show representative tapping mode AFM, and Fig. 4e and f show SEM micrographs of the chitosan/insulin nanoparticles and DCTS/insulin self-assembled nanoparticles, respectively. Almost all of the nanoparticles are of compact structure, having spherical or subspherical shape with smooth surface. The diameter of the DCTS/insulin self-assembled nanoparticles is roughly within the range of 65–100 nm (Fig. 4d and f), much smaller than unmodified chitosan insulin nanoparticles of 90–120 nm size (Fig. 4c and e) at the same weight ratio, which is quite consistent with the DLS measurement. Furthermore, the higher number of cationic charges offered by DCTS (due to grafting of PAMAM) is able to tightly condense higher amounts of negatively charged insulin to form smaller particles than native chitosan. The micrographs also demonstrate that the nanocomplexes are scattered independently over the field, suggesting possible stabilization against self-aggregation. Our previous reports also showed similar results.[6] SEM images of self-assembled nanocomplexes also show that the polyplexes are spherical in shape, and the particle size is in the range of 65–100 nm, which is also in good agreement with the AFM micrographs. These results are very similar to the previously reported ones.[23] The above results confirm that the dendronized chitosan is more capable of condensing significant amounts of insulin into nanoparticles of sufficiently small sizes for uptake by intestinal epithelial cells.

3.4. Insulin loading capacity and insulin encapsulation efficiency

Encapsulation and loading capacity of insulin is another important aspect in oral delivery. Poor encapsulation efficiency restricts the wide use of polymeric carriers, as they would be unable to pursue the desired function after administration. Therefore, the percentage of insulin loading capacity and insulin encapsulation of the nanoparticles with different weight ratios (0.5 : 1, 1 : 1 and 2 : 1) was investigated, as shown in Fig. 5a and b. Insulin loading capacity of chitosan/insulin nanoparticles at different weight ratios varies between 15–22%, and the encapsulation efficiency of chitosan/insulin nanoparticles at 0.5 : 1, 1 : 1 and 2 : 1 weight ratios are 63%, 78% and 86%, respectively; whereas DCTS/insulin nanoparticles at these weight ratios showed better insulin loading (22–27%) as well as insulin encapsulation efficiency of 74%, 89% and 95%. As DCTS carries more cationic charges over unmodified chitosan, stronger ionic interaction between the negative charges of insulin and the positive charges of DCTS may induce better loading capacity and improved insulin encapsulation.

3.5. *In vitro* insulin release profile in simulated gastric fluid (SGF) and simulated intestinal fluid (SIF)

The cumulative release profiles of insulin from DCTS/insulin nanocomplexes were investigated in pH gradients corresponding to the gastrointestinal tract, *i.e.*, pH 2.0 (simulated gastric fluid, SGF) and pH 7.4 (simulated intestinal fluid, SIF) at 37 ± 0.5 °C. The amount of released insulin is measured by UV spectrophotometer at 280 nm, as shown in Fig. 5c. It is observed that in SGF, at pH 1.2, chitosan/insulin self-assembled nanoparticles retard the immediate release of insulin, releasing only ~16% of the encapsulated insulin in the initial 2 h, while DCTS/insulin self-assembled nanoparticles show better protection of insulin, releasing only ~10% for the same period of time. As insulin is more strongly bound to DCTS due to the presence of more positively charged amines compared to chitosan, there is less possibility of penetration of acidic media and thereby less release of insulin from DCTS/insulin nanoparticles. The residual protonated amines in both chitosan and DCTS do not allow them to interact with the protonated medium, as charges of similar nature repulse. On the contrary, in SIF (pH 7.4), the amount of released insulin from the native chitosan/insulin self-assembled nanocomplexes is about 82% of the encapsulated amount. After the first hour, only ~28% insulin release is observed, which reaches >74% on the 5th h. On the other hand, DCTS/insulin self-assembled nanoparticles show more sustained insulin release, where initially (1–2 h), 40–50% of insulin is released, but above 90% of insulin is released after 6 h of incubation. The presence of residual positive charges in both chitosan and DCTS (these are available even after their partial neutralization with insulin) allow them to interact with the moderately alkaline medium, which thereby penetrates these nanoparticles, leading to more release of insulin in SIF compared to SGF (Fig. 5c). Thus, the pH-responsive, prolonged release pattern of insulin can facilitate its oral administration in the animal model, minimising the chances of hypoglycemia. The mathematical analysis also shows the diffusion-controlled and the swelling-controlled insulin release pattern from the nanoparticles. Results related to experiments in the pH gradient medium are shown in Table 2. It is noted from the obtained correlation coefficient values ($R \geq 0.99$) that the release data fit well to the empirical equation. The "n" release exponent ranged from 0.53 to 0.78 (Table 2), indicating a non-Fickian (anomalous) transport ($0.45 < n < 0.89$) for all the tested nanoparticle samples.[19,20] So, the results indicate both diffusion-controlled as well as swelling-controlled insulin release (anomalous transport or non-Fickian diffusion mechanism) from the self-assembled nanoparticles.

Fig. 5d demonstrates the significant mucoadhesive property of the DCTS/insulin self-assembled nanoparticles, which

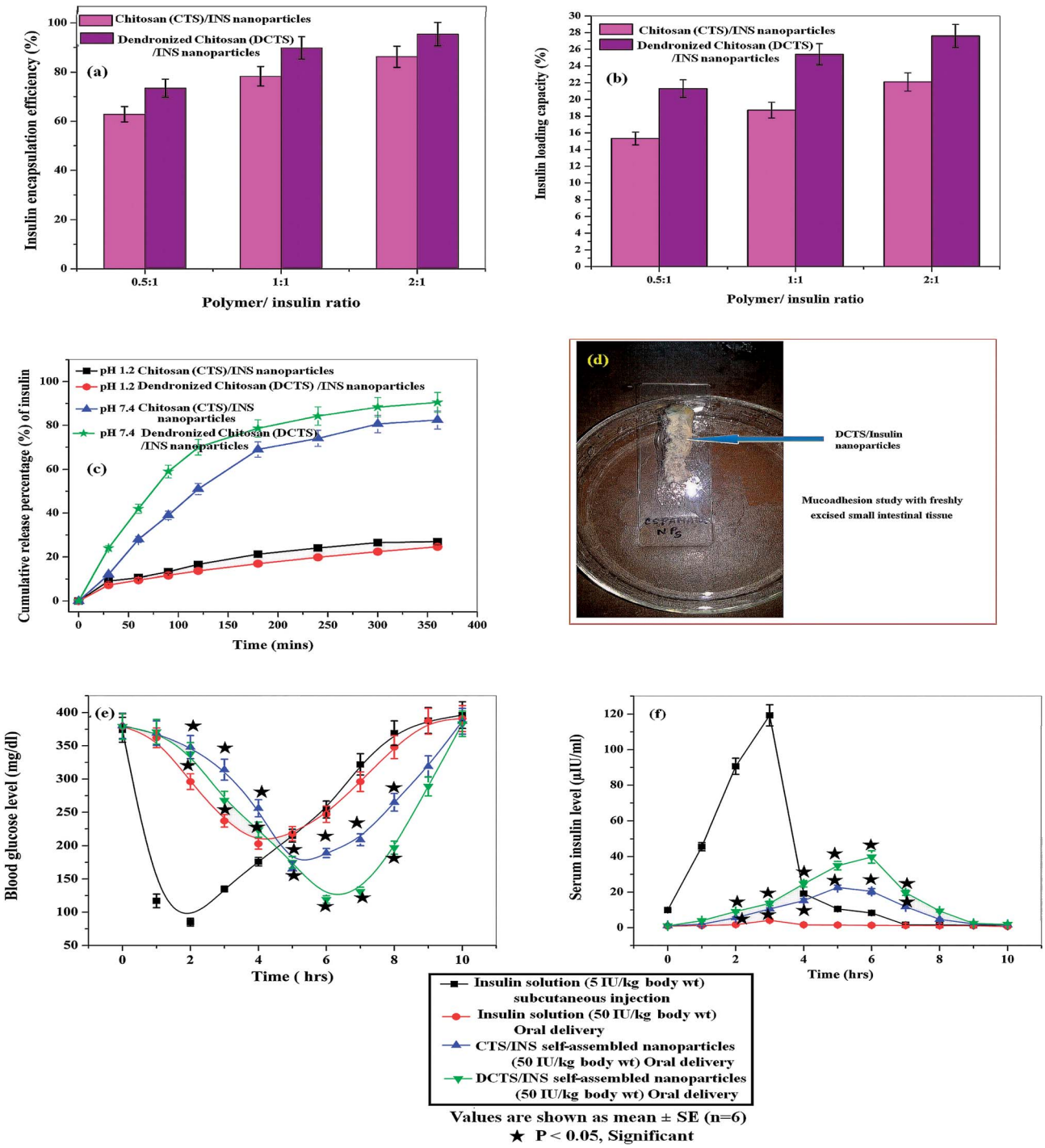

Fig. 5 (a) Percentage of insulin encapsulation, (b) insulin loading capacity, (c) cumulative insulin release profile, (d) mucoadhesion study in excised animal tissue, (e) *in vivo* pharmacological response and (f) serum insulin concentration after peroral treatment of self-assembled nanoparticles.

remained attached to the mouse intestinal lumen after continuous washing with buffer (pH 7.4) for 30 min. The mucoadhesive features of the nanoparticles could be attributed to an interaction between the positive charged amino groups of dendronized chitosan and the negatively charged sialic acid groups of mucin, which provides a prolonged interaction within the intestinal mucosa. Hence, the mucoadhesive nanoparticles have strong electrostatic interaction with the negative charged mucous layer, offering prolonged resident time and helping sustained release of the encapsulated insulin. Moreover, increased paracellular permeability could be achieved by redistribution of F-actin and the tight junction's protein through the interaction between the positively charged nanoparticles with the negatively charged cell surfaces and tight junctions.

Table 2 Estimated parameters and drug release mechanism of self-assembled nanoparticles

Sample	Zero-order r^2	First-order r^2	Higuchi r^2	Korsmeyer–Peppas r^2	Korsmeyer–Peppas n	Drug transport mechanism
pH 1.2						
CS/insulin nanoparticles	0.8968	0.9215	0.9891	0.9921	0.5651	Non-Fickian
DCTS/insulin nanoparticles	0.9295	0.9503	0.9983	0.998	0.5396	Non-Fickian
pH 7.4						
CS/insulin nanoparticles	0.893	0.9785	0.9644	0.9895	0.7826	Non-Fickian
DCTS/insulin nanoparticles	0.7912	0.9662	0.9515	0.9665	0.7822	Non-Fickian

3.6. *In vivo* pharmacological response

In vivo pharmacological responses of DCTS/insulin self-assembled nanoparticles after peroral treatment in diabetic mice are illustrated in Fig. 5e. Both chitosan/insulin and DCTS/insulin self-assembled nanoparticles show hypoglycemic effects after oral delivery, as compared to the control (subcutaneous injection of insulin 5 IU kg^{-1} b.w.). But DCTS/insulin self-assembled nanoparticles exhibit more pronounced effects in the lowering of blood glucose level compared to native chitosan nanoparticles. After subcutaneous injection, the blood glucose level starts decreasing significantly within 30–45 min and reaches 85 mg dL^{-1} at the 2nd h post-administration. However, the hypoglycemic effect is further sustained for only 2 h and subsequently returns to its basal level at the 5th h of administration (Fig. 5e). On the other hand, oral administration of chitosan/insulin self-assembled nanoparticles and DCTS/insulin self-assembled nanoparticles (both 50 IU kg^{-1} b.w.) result in the significant reduction of glycemia. In the case of these nanoparticles, the reduction in the glucose level in diabetic mice is initiated after 2–3 h of administration. However, DCTS/insulin self-assembled nanoparticles show sustained hypoglycemic effects for 8 h, reducing the blood glucose level up to 119 mg dL^{-1}. On the other hand, chitosan/insulin nanoparticles lower the glucose level down to 165 mg dL^{-1} at the 5th h, and the effects sustain only for another 30 min to an hour.

The corresponding serum insulin concentrations at different time profiles were studied and are shown in Fig. 5f. It is observed that the subcutaneous injection of insulin solution (5 IU kg^{-1} b.w.) results in the maximum serum insulin concentration at the 3rd h post-injection, whereas the oral administration of chitosan/insulin self-assembled nanoparticles at a dose of 50 IU kg^{-1} b.w. shows the maximum concentration of serum insulin at the 5th h of administration. Again, DCTS/insulin self-assembled nanoparticles exhibit the maximum serum insulin at the 6th h post-administration. In contrast, a negligible amount of serum insulin (bovine insulin) is detected in animals treated perorally with insulin solution. From the $AUC_{(0-10h)}$ data of the DCTS/insulin nanoparticle-orally treated mice, the relative bioavailability (RA) is found to be ~9.19%, where the RA of chitosan/insulin nanoparticles is only ~5.28%.

Orally administered DCTS/insulin nanoparticles remain biologically active and show prolonged hypoglycemic effects for 2–8 h (Fig. 5e) without producing any sudden hypoglycemic shock in diabetic mice. However, the administration of free oral insulin solution does not have any pronounced effect on glycemia. The relative availability (RA) of insulin was found to be ~9.19% with DCTS/insulin nanoparticles, which is almost double that of native chitosan/insulin nanoparticles (~5.28%), suggesting significant absorption of insulin in an active form. Bioavailability for oral insulin trials has been reported to be low, as only <2.5% insulin bioavailability has been documented with pH-responsive poly(methacrylic-*g*-ethylene glycol) hydrogel microparticles in oral delivery;[25] ~4% bioavailability has been reported with chitosan nanoparticles;[26] 7% of bioavailability is observed in Alg/Chit nanoparticles;[23] ~4.43% insulin bioavailability was found in our previous study using *N*-succinyl chitosan grafted polyacrylamide hydrogels;[21] and ~8.11% of bioavailability was found using core shell nanoparticles.[27] In the present investigation, the encapsulated insulin is well protected from enzymatic degradation, as it is sheltered within the nanoparticles. As enzymes (pepsin and trypsin) in the GI tract are positively charged species, they cannot bind to the positively charged nanoparticles. Therefore, an intimate contact of the nanoparticles with the intestinal wall is established, allowing a significant amount of insulin absorption, although some amount of the released insulin is probably damaged by the classical degradation phenomena during its transit through the GI tract. While the zwitterionic chitosan/PAMAM complex has been reported as a potential drug carrier to solid tumors,[28] in the present investigation, self-assembled nanoparticles of PAMAM-grafted chitosan for oral insulin delivery showed excellent hypoglycemic effects in *in vivo* model.

3.7. Evaluation of *in vivo* toxicity after oral administration of dendronized chitosan (DCTS)

3.7.1. Minimum lethal dose (MLD). No lethality is observed up to 300 mg kg^{-1} b.w. of DCTS nanoparticles at peroral dose.

3.7.2. Liver function test analysis. The liver-specific enzymes ASAT (asparate aminotransferase) and ALAT (alanine aminotransferase) are significantly elevated in hepatobilliary diseases with a direct correlation with liver parenchyma damage. As shown in Fig. 6a, the SGOT value is 64.8 U L^{-1} for the control animal and 94.8 U L^{-1} and 114.75 U L^{-1} for the animals treated with chitosan nanoparticles and DCTS nanoparticles (300 mg kg^{-1} b.w.), respectively. These values are within the reference range of SGOT (55–251 U L^{-1}) for mouse.

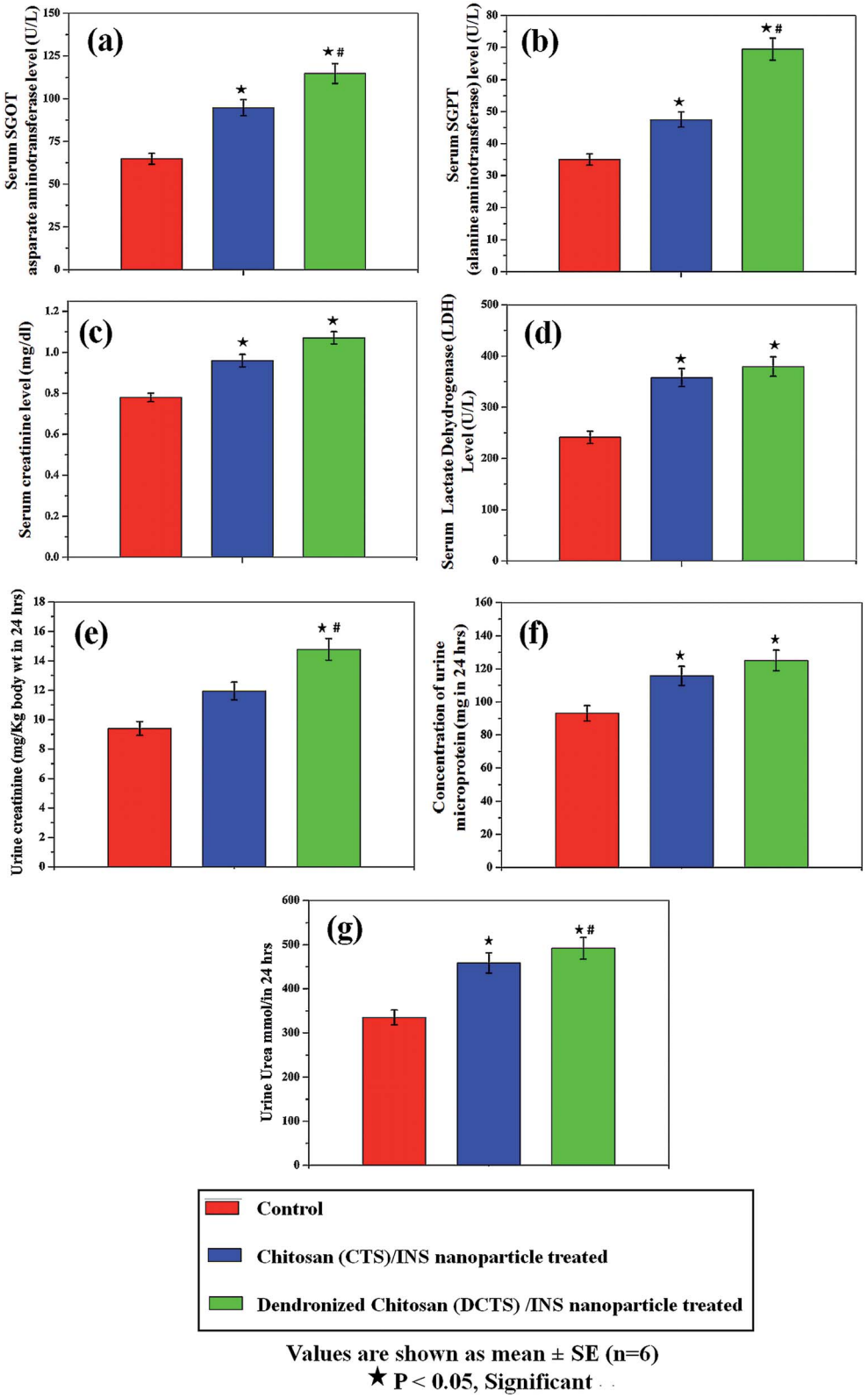

Fig. 6 Acute toxicity study of DCTS nanoparticle-treated animals, (a) serum SGOT, (b) serum SGPT, (c) serum creatinine, (d) serum LDH, (e) urine creatinine, (f) urine microprotein and (g) urine urea.

Again, Fig. 6b shows that the SGPT value is 35.02 U L^{-1} for the control animals, 47.5 U L^{-1} for the animals treated with chitosan nanoparticles, and 69.45 U L^{-1} for the animals treated with DCTS nanoparticles. The values are within the reference range of 28–184 U L^{-1} in mouse. The serum creatinine level is 0.42 mg dL^{-1} for the control animal, 0.61 mg dL^{-1} for the animals

treated with chitosan nanoparticles and 0.67 mg dL^{-1} for the animals treated with DCTS nanoparticles (Fig. 6c), where the normal reference range is 0.7–1.1 mg dL^{-1}. Again, the LDH value (Fig. 6d) is 241.2 U L^{-1} for the control animal, 358.1 U L^{-1} for animals treated with chitosan nanoparticles and 379.7 U L^{-1} for the animals treated with DCTS nanoparticles; these values are within the normal reference range of 230–460 U L^{-1}. Although significant changes in SGPT, SGOT and LDH values are found in comparison to the control, all these values are within the reference range, suggesting no damage of the liver, and no toxicological and functional disorder in the animal by the treatment of DCTS nanoparticles.

3.7.3. Assessment of nephro-toxicity. Urine creatinine is an indicator of the urinary tract obstruction, kidney failure, dehydration, severe kidney disease, shock, renal outflow obstruction and acute tubular necrosis. Therefore, the concentration of urine creatinine was measured and is reported in Fig. 6e. The creatinine value in control mice is 9.4 mg kg^{-1} b.w., it is 14.79 and 11.95 mg kg^{-1} b.w. in mice treated with DCTS and chitosan nanoparticles (300 mg kg^{-1} b.w.), respectively. The values fall within the reference range of 8.4–24.6 mg kg^{-1} b.w. Furthermore, proteins (albumin and globulin fractions) are known to be involved in the maintenance of the normal distribution of water between the blood and the tissues. Mainly, proteinuria occurs with increased glomerular permeability or defective tubular reabsorption. Therefore, the concentration of urine microprotein could be an indicator of renal disease or any glomerular damage, and increased urea is generally accompanied by renal damage. Fig. 6f shows that the concentration of urine microprotein is 93 mg per 24 h for the control animal, 115.7 mg per 24 h for the animals treated with chitosan nanoparticles and 125.1 mg per 24 h for those treated with DCTS nanoparticles. A significant change is found in comparison to the control group, but the microprotein values are within normal reference range of 28–140 mg per 24 h. The concentration of urea in urine was also measured and is presented in Fig. 6g. The urea concentration is 491.8 mmol in 24 h for the animals treated with DCTS nanoparticles (300 mg kg^{-1} b.w.) and 458.6 mmol in 24 h for those treated with chitosan nanoparticles. A significant change is observed as compared to the control animal group (335 mmol in 24 h), although these values are within the reference range of 333–583 mmol per 24 h. Thus,

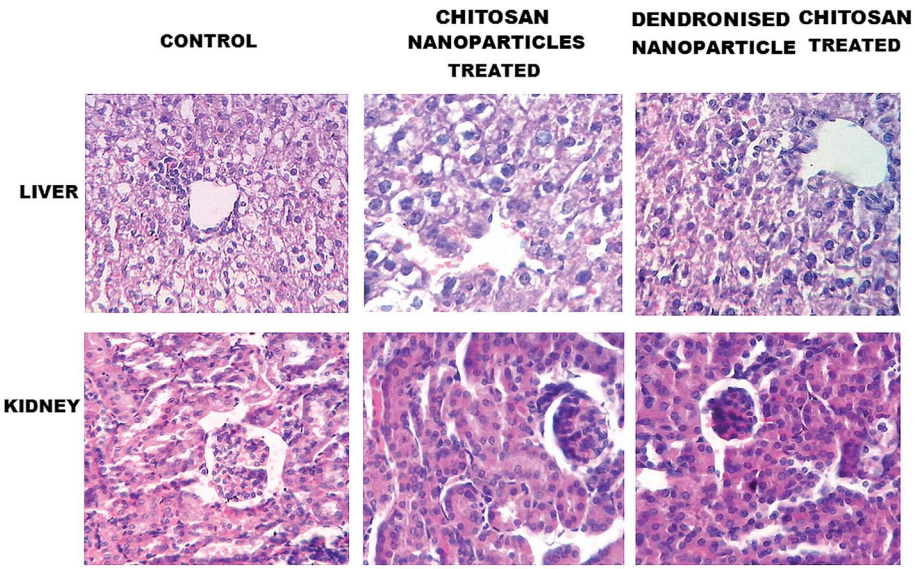

Fig. 7 Sections of liver and kidney (H&E staining, magnification 40×) of control and treated (peroral chitosan and DCTS nanoparticles) mice.

Table 3 Qualitative analysis of different biochemical parameters of urine in polymeric nanoparticle-treated animals

Parameters	Control animal (treated with 0.9% NaCl)	Peroral treatment with chitosan nanoparticles (300 mg Kg^{-1} b.w)	Peroral treatment with dendronized chitosan nanoparticles (300 mg Kg^{-1} b.w)
Urobilinogen	0.2	1	0.2
Protein	Negligible	Trace	Negligible
pH	7.5	7.5	8.0
Blood	Moderate (non-haemolysed)	Moderate (haemolysed)	Trace (haemolysed)
Specific gravity	1.015	1.020	1.005
Ketone	15–30	40	Negligible
Bilirubin	Negligible	+	Negligible
Glucose	Negligible	Negligible	Negligible

all these studies indicate that DCTS can be a safe polymer for oral insulin delivery, indicating no renal dysfunction.

3.8. Pathohistological diagnosis

No gross histopathological changes in liver and kidney sections (Fig. 7) were observed. The liver sections (H&E staining) of the treated animal group exhibit a central vein with the radiating hepatic cells, similar to the control tissue. The sections of the kidney also show the renal corpuscles surrounded by Bowman's capsule and kidney tubules, lined by the simple cuboidal epithelium. A urinary space (appearing as a clear space) is also visible on the histological slides. The glomerulus (tuft of capillaries) appears as a large cellular mass, implying no hepatic or renal toxicity in the animal model. Furthermore, qualitative analyses of different biochemical parameters (Table 3) also indicate its safety measures.

4. Conclusions

A low-toxicity, pH-sensitive, water-soluble chitosan derivative was successfully prepared for oral insulin delivery. The self-assembled nanoparticles with ~27% insulin loading and ~95% insulin encapsulation efficiency are prepared through a mild process, avoiding harmful chemicals. The pH-responsive nanoparticles are able to establish a prolonged hypoglycemic effect compared to those obtained from oral insulin and native chitosan nanoparticles, revealing an almost doubly-enhanced insulin bioavailability (~9.19%) compared to native chitosan nanoparticles (~5.28%). Since no systemic toxicity is observed in experimental trials, one is assured that the dendronized chitosan can be a promising polymeric vehicle in oral insulin or other therapeutic drugs due to its efficient and safe administration.

Acknowledgements

We are highly grateful to the Department of Science and Technology, Government of West Bengal for their financial support for this work and the project entitled '*Synthesis of derivatives of chitosan and their IPNs for oral insulin delivery*'; Sanction no. 428 (Sanc./ST/P/S & T/2G-7/2011).

Notes and references

1 P. Mukhopadhyay, R. Mishra, D. Rana and P. P. Kundu, *Prog. Polym. Sci.*, 2012, **37**, 1457.
2 R. Mo, T. Jiang, J. Di, W. Tai and Z. Gu, *Chem. Soc. Rev.*, 2014, **43**, 3595.
3 K. Bowman and K. W. Leong, *Int. J. Nanomed.*, 2006, **1**, 117.
4 P. Mukhopadhyay, K. Sarkar, S. Soam and P. P. Kundu, *J. Appl. Polym. Sci.*, 2013, **129**, 835.
5 K. Sarkar and P. P. Kundu, *Int. J. Biol. Macromol.*, 2012, **51**, 859.
6 P. Mukhopadhyay, K. Sarkar, M. Chakraborty, S. Bhattacharya, R. Mishra and P. P. Kundu, *Mater. Sci. Eng., C*, 2013, **33**, 376.
7 E. A. Stepnova, V. E. Tikhonov, T. A. Babushkina, T. P. Klimova, E. V. Vorontsov, V. G. Babak, S. A. Lopatin and I. A. Yamskov, *Eur. Polym. J.*, 2007, **43**, 2414.
8 R. A. A. Muzzarelli and F. Tanfani, *Carbohydr. Polym.*, 1985, **5**, 297.
9 H. Sashiwa, N. Kawasaki, A. Nakayama, E. Muraki, N. Yamamoto and S. I. Aiba, *Biomacromolecules*, 2002, **3**, 1126.
10 R. Esfand and D. A. Tomalia, *Drug Discovery Today*, 2001, **6**, 427.
11 S. Svenson and D. A. Tomalia, *Adv. Drug Delivery Rev.*, 2005, **57**, 2106.
12 K. Sarkar, M. Debnath and P. P. Kundu, *Carbohydr. Polym.*, 2013, **92**, 2048.
13 R. Duncan and L. Izzo, *Adv. Drug Delivery Rev.*, 2005, **57**, 2215.
14 K. Sarkar and P. P. Kundu, *Carbohydr. Polym.*, 2013, **98**, 495.
15 H. Sashiwa, Y. Shigemasa and R. Roy, *Macromolecules*, 2000, **33**, 6913.
16 H. Sashiwa, Y. Shigemasa and R. Roy, *Carbohydr. Polym.*, 2002, **49**, 195.
17 D. A. Tomalia, H. Baker, J. Dewald, M. Hall, G. Kallos, S. Martin, J. Roek, J. Ryder and P. Smith, *Polym. J.*, 1985, **17**, 117.
18 H. Sashiwa, Y. Shigemasa and R. Roy, *Carbohydr. Polym.*, 2002, **47**, 201.
19 P. L. Ritger and N. A. Peppas, *J. Controlled Release*, 1987, **5**, 37.
20 X. Zhang, Z. Wu, X. Gao, S. Shu, H. Zhang and Z. Wang, *Carbohydr. Polym.*, 2009, **2**, 394.
21 P. Mukhopadhyay, K. Sarkar, S. Bhattacharya, A. Bhattacharyya, R. Mishra and P. P. Kundu, *Carbohydr. Polym.*, 2014, **112**, 627.
22 F. Cui, K. Shi, L. Zhang, A. Tao and Y. Kawashima, *J. Controlled Release*, 2006, **114**, 242.
23 B. Sarmento, A. Ribeiro, F. Veiga, P. Sampaio, R. Neufeld and D. Ferreira, *Pharmacol. Res.*, 2007, **24**, 2198.
24 Y. Pan, Y. J. Li, H. Y. Zhao, J. M. Zheng, H. Xu, G. Wei, J. S. Hao and F. D. Cui, *Int. J. Pharm.*, 2002, **249**, 139.
25 A. M. Lowman, M. Morishita, M. Kajita, T. Nagai and N. A. Peppas, *Int. J. Pharm.*, 1999, **88**, 933.
26 Z. Ma, T. M. Lim and L. Y. Lim, *Int. J. Pharm.*, 2005, **293**, 271.
27 P. Mukhopadhyay, S. Chakraborty, S. Bhattacharya, R. Mishra and P. P. Kundu, *Int. J. Biol. Macromol.*, 2014, accepted manuscript.
28 K. C. Liu and Y. Yeo, *Mol. Pharm.*, 2013, **10**, 1695.

